Full-Wave Analysis of Indoor Electromagnetic Pollution from Base-Station Antennas

Xunwang Zhao, Zhongchao Lin, Huanhuan Zhang, Sio-Weng Ting, and Yu Zhang

School of Electronic Engineering
Collaborate Innovation Center of Information Sensing and Understanding
Xidian University, Xi'an, Shaanxi 710071, China
zhanghuanajkd@outlook.com, xdzxw@126.com

Abstract ─ Three-dimensional (3D) intricately detailed models for base-station antennas and buildings are created. Indoor radiation from antennas is accurately analyzed using the higher-order basis functions (HOBs) in the context of method of moments (MoM). The use of HOBs reduces the number of unknowns in MoM compared with the use of piecewise Rao-Wilton-Glisson basis functions (RWGs). To significantly improve the capability of MoM, an efficient parallel algorithm is developed based on a block-cyclic matrix distribution scheme. Taking radiation power, main-beam pointing and materials into account, the electric-field distribution inside buildings is simulated to determine the indoor radiation level, which may be beyond the safety limit. The numerical results are verified through comparison with the measured results.

Index Terms ─ Base-station antennas, buildings, radiation safety, method of moments, parallel technique.

I. INTRODUCTION

More and more base stations for mobile communication systems are built to achieve better signal coverage, as shown in Fig. 1. On the other hand, the strength of electromagnetic field from base stations can be too strong to exceed the safety limit, which is referred to as electromagnetic pollution. It is an electromagnetic compatibility (EMC) problem becoming a matter of concern for more and more people. Therefore, it is necessary to assess the radiation in urban buildings.

Since measurements with electromagnetic meters or other tools are costly to identify the radiation level [1, 2], the approach based on electromagnetic simulation can be applied. Moreover, the use of computational methods can calculate the field strength at a point where measurement is difficult to be undertaken. Among various methods, the ray-tracing technique is widely used for predicting channel capacity or path loss in indoor environment because this kind of high-frequency asymptotic method is low-cost in simulation of electrically large structures [3, 4]. However, as is known, it is not accurate for complex models including thin geometric structures.

Fig. 1. Base-station antennas on a building.

To obtain accurate results, full-wave methods, such as the method of moments (MoM) [5] and the finite-difference time-domain (FDTD) method [6], are also employed for indoor channel capacity [7–9]. This kind of methods requires a large amount of data regarding geometries, building locations, materials, and so on, and is computationally intensive. It is not convenient for FDTD to simulate open-region problems because FDTD needs absorbing boundary condition. Due to the high computational complexity and memory requirement, it is difficult for MoM to solve electrically large problems. Therefore, the MoM-based fast algorithm, namely multilevel fast multipole algorithm (MLFMA), has been utilized to compute electric-field (E-field) distribution in indoor environment [10]. However, since buildings contain complex structures and multiple dielectrics, low convergence or even divergence usually occurs for MLFMA.

In addition, there is a kind of empirical (statistical) methods including Hata model, COST-231-Walfisch-Ikegami model and dual-slope model. The interested readers are referred to [4, 11] for a summarization of these methods for indoor propagation. These methods are based on the statistical characterization of the received signals. They are easier to implement and require less computational effort, but less accurate than

Submitted On: March 6, 2016
Accepted On: May 27, 2016

numerical methods.

Previous works mainly deal with two-dimensional (2D) buildings and focused on channel capacity and path loss. In this paper, we use MoM with the higher-order basis functions (HOBs) to analyze indoor E-field distribution and extend full-wave analysis to 3D scenarios. The concern is the safety of indoor radiation rather than channel capacity and path loss. The high-performance parallel computing technique is utilized to greatly improve the capability of MoM. Multiple factors including radiation power, main-beam pointing and materials are taken into account to determine whether the radiation level exceeds the safety limit or not.

II. PARALLEL HIGHER-ORDER METHOD OF MOMENTS

A. Integral equations

Base-station antennas and buildings contain metallic and dielectric materials, and a general form of the Poggio–Miller–Chang–Harrington–Wu (PMCHW) formulation is utilized [12, 13], which is solved in frequency domain for equivalent electric and magnetic currents over dielectric boundary surfaces and electric currents over perfect electric conductors (PECs). The set of integral equations are solved by using MoM, specifically the Galerkin's method.

For the case when one of the two domains sharing a common boundary surface is a PEC, the magnetic currents are equal to zero at the boundary surface and therefore, the PMCHW formulation degenerates into the electric field integral equation (EFIE).

B. Higher-order basis functions

Higher-order polynomials over bilinear quadrilateral patches are used as basis functions over relatively large subdomains [12],

$$\boldsymbol{F}_{ij}(p,s) = \frac{\boldsymbol{\alpha}_s}{\left|\boldsymbol{\alpha}_p \times \boldsymbol{\alpha}_s\right|} p^i s^j,\ -1 \le p \le 1,\ -1 \le s \le 1, \quad (1)$$

where, p and s are local coordinates, i and j are orders of basis functions, and $\boldsymbol{\alpha}_p$ and $\boldsymbol{\alpha}_s$ are covariant unitary vectors. A quadrilateral patch is illustrated in Fig. 2.

The orders can be adjusted according to the electrical size of a geometric element. The orders increase as the element becomes larger. The electrical size of a geometric element can be as large as two wavelengths. Typically, the number of unknowns for HOBs is reduced by a factor of 5–10 compared with that for traditional piecewise basis functions, e.g. Rao-Wilton-Glisson basis functions (RWGs) [14], and thus the use of HOBs drastically reduces the computational amount and memory requirement. Note that the polynomials can also be used as basis functions for wire structures. In this case, truncated cones are used for geometric modeling [12].

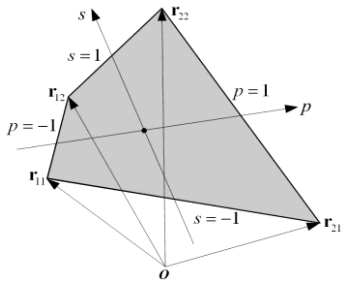

Fig. 2. Bilinear quadrilateral patch defined by four vertices with the position vectors $\boldsymbol{r}_{11}$, $\boldsymbol{r}_{21}$, $\boldsymbol{r}_{12}$ and $\boldsymbol{r}_{22}$.

C. Parallel technique

The parallel scheme for MoM is partitioning the dense complex matrix. The large dense MoM matrix is divided into a number of smaller block matrices that are nearly equal in size and distributed among all participating processes, assuming that each parallel process runs on one CPU core here. The distribution manner of the blocks is chosen appropriately according to the parallel LU decomposition solver to minimize the communication between processes. Specifically, a block-cyclic matrix distribution is used among processes. Two factors, process grid and block size, significantly affects the performance of the parallel algorithm [15]. Setting the shape of process grid $P_r \times P_c$ as square as possible, with P_c slightly larger, enables the algorithm implementation to be most efficient. The block size depends on the CPU cache size and needs to be tested on computational platforms to determine the optimum value. The typical value of the block size for modern CPUs is 128.

III. SAFETY LIMIT OF BASE-STATION RADIATION

The International Commission on Non-Ionizing Radiation Protection (ICNIRP) has defined the guideline for limiting electromagnetic radiation exposure and provided protection against known adverse health effects, which is a popular reference standard in many countries. The ICNIRP standard in the frequency range from 400 MHz to 2000 MHz is given in Table 1. According to this standard, the threshold of E-field strength at 900 MHz is 41.2 V/m corresponding to 4.5 W/m^2. An even tougher standard is adopted in China, which is 12.0 V/m corresponding to 0.4 W/m^2, as shown in Table 1.

Table 1: Threshold of radiation level

Country/Region	E-field Strength (V/m)	Power Density (W/m^2)
ICNIRP (400 MHz−2000 MHz)	$1.375\, f^{1/2}$	$f/200$
China (30 MHz−3000 MHz)	12.0	0.4

IV. ANALYSIS OF E-FIELD DISTRIBUTION IN BUILDINGS

A base-station antenna working at 944 MHz is created first. Then the E-field distribution generated by two base-station antennas inside a smaller apartment (denoted by Apartment I) is simulated and compared with the measured results for verification. Finally, two base-station antennas radiating E-field inside a larger apartment (denoted by Apartment II) are simulated and analyzed.

A. Modeling of the base-station antenna

The base-station antenna consists of five cross-dipole elements and a back plate, as shown in Fig. 3. The tilt angle of the dipole is ±45°. The length of each dipole is 0.168 m and the distance between two neighboring antenna elements is 0.246 m. Each dipole is excited by a delta-gap voltage source. The working frequency of the antenna is 944 MHz. The red arrows in Fig. 3 denote the locations of the sources. The radiation patterns of the antenna are simulated by the proposed higher-order MoM and the FEKO software [16]. Note that FEKO uses the traditional piecewise basis functions, such as the RWG basis functions. The number of unknowns for HOBs is 831 and that for FEKO is 4000. Since the antenna is a small model, we do not use the parallel algorithm in this simulation. The total simulation time for HOBs is 16.4 s and that for FEKO is 37.0 s. The radiation patterns of the antenna are compared in Fig. 4. The results from HOBs agree well with those from FEKO, but the number of unknowns and simulation time for HOBs are much lower. Figure 5 shows the 3D radiation pattern of the antenna that will be used in the following examples.

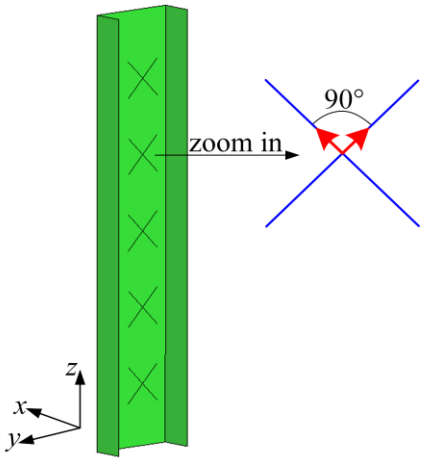

Fig. 3. Base-station antenna and its cross-dipole elements.

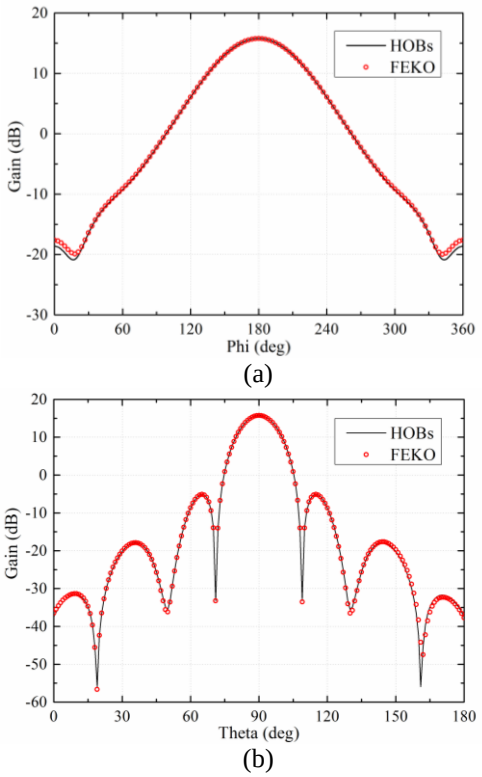

Fig. 4. Radiation patterns of the base-station antenna in: (a) the *xoy* plane and (b) the *xoz* plane.

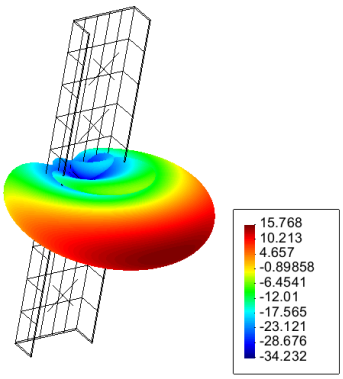

Fig. 5. 3D radiation pattern of the base-station antenna.

B. E-field distribution in Apartment I

Two base-station antennas are installed in front of an apartment denoted by Apartment I [17], which is a real building located at University of Macau. The main-lobes of the two antennas are pointed to different directions, as shown in Fig. 6 (a). In detail, the main-lobe direction of Antenna 1 is ϕ=45° and θ=90°, and that of Antenna 2 is ϕ=0° and θ=102°. The radiation power of each antenna is 365 mW. The antenna

locations and the apartment dimensions are demonstrated in Fig. 6 (b). The wall, ceiling and floor of the apartment are assumed to be homogeneous dielectrics. They are made of concrete with equivalent permittivity ε_r=3.916 and have a thickness of 0.2 m. The thickness of the door and windows, which are made of glass (ε_r=2.37), is 0.012 m.

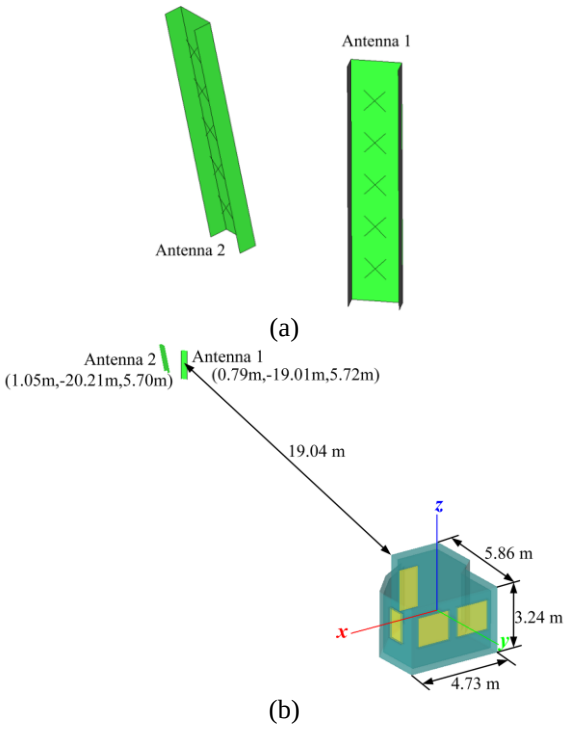

Fig. 6. Two base-station antennas in front of Apartment I: (a) two base-station antennas with different main-beam directions and (b) locations of the base-station antennas and dimensions of Apartment I. The wall, ceiling and floor of the apartment are in dark green color, and the door and windows in yellow color.

The number of unknowns for this model is 311,261. The computing platform used in this simulation is the Magic Cube with 1450 nodes at Shanghai Supercomputer Center (SSC), and each node has four quad-core 1.9 GHz processors and 64 GB memory (http://www.ssc.net.cn/en/ resources_1.aspx). The total simulation time is about 11.8 hours when 512 CPU cores are used and the memory required is about 1.4 TB. The radiation pattern and E-field distribution are shown in Fig. 7. The E-field at four points inside the apartment is compared with the measured results, as listed in Table 2. The tool for measurement was a mobile phone installed with a commercial mobile network measurement software called NEMO [18]. From comparison, it is observed that the computed and measured fields agree with each other.

It can be seen from Fig. 7 that the maximum value of E-field strength is approximately 1.4 V/m, which is below both the ICNIRP and China standards. There are several factors that affect the indoor radiation level: (1) radiation power of antennas, (2) gain of antennas, (3) distance between antennas and buildings and (4) materials of buildings. In this simulation, the radiation power is low and the main lobe is not directly pointed to the apartment, and therefore, the indoor radiation is weak.

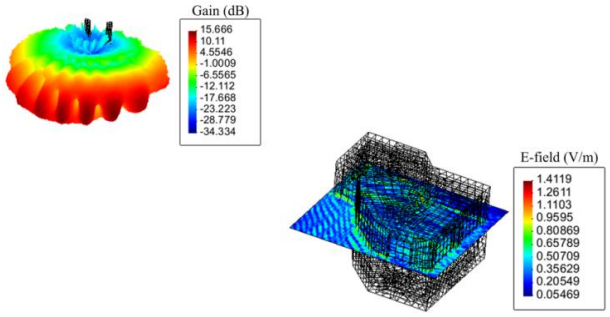

Fig. 7. Radiation pattern of the base-station antennas and the E-field distribution on a cut-plane at a height of 1.70 m inside and around Apartment I.

Table 2: Comparison of simulated and measured E-field in Apartment I

Location (m)	Simulation (V/m)	Measurement (V/m)
(3.24, 2.98, 1.70)	0.38	0.536
(4.55, 4.47, 1.70)	0.34	0.393
(1.75, 4.36, 1.70)	0.45	0.474
(1.09, 1.69, 1.70)	0.88	0.927

C. E-field distribution in Apartment II

Consider two base-station antennas in front of a larger apartment denoted by Apartment II. The distance between the two antenna centers is 1.28 m and both the antennas are tilted 12° in the vertical plane, as shown in Fig. 8 (a). The radiation power of each antenna is 10 W, which is much higher than that in last section. The locations of the antennas and the dimensions of the apartment are demonstrated in Fig. 8 (b). The thickness of the wall, ceiling and floor is 0.16 m, and that of the door and windows is 0.003 m. The dielectric permittivity of the apartment is the same as that in last section, but the conductivity of the wall, ceiling and floor is set as 0.002 S/m.

The number of unknowns is 1,179,986, which is challenging for MoM. To facilitate the simulation, we set the *xoz* plane as a symmetry plane and the number of unknowns is reduced by half. The computing cluster used here has 136 nodes at Xidian University, and each

node has two 12-core 2.2 GHz processors and 64 GB memory. The total simulation time is about 6 hours when 2400 CPU cores are used and the memory required is about 5.1 TB.

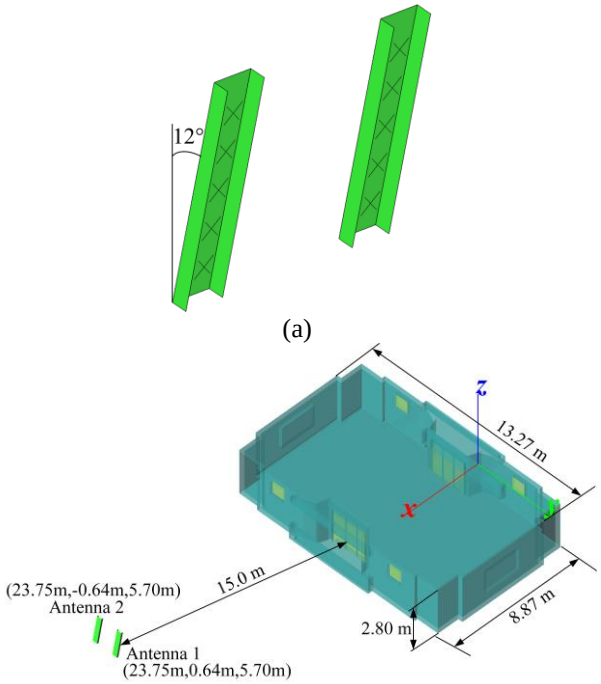

Fig. 8. Two base-station antennas in front of Apartment II: (a) attitude of the two base-station antennas and (b) locations of the base-station antennas and dimensions of Apartment II. The wall, ceiling and floor of the apartment are denoted in dark green color, and the doors and windows in yellow color.

The radiation pattern and E-field distribution are shown in Fig. 9. It is obvious that the maximum value of E-field strength is nearly 26 V/m, which is still below the ICNIRP standard. However, it is higher than twice the China standard.

To reduce the E-field strength inside Apartment II, a simple approach is to reduce the radiation power of antennas. However, it would reduce the signal coverage of base stations. Instead, we change the main-lobe directions by rotating the antennas in the azimuth plane, which is equivalent to the reduction of the antenna gain. As shown in Fig. 10, the angle is denoted by α. We consider three different azimuth angles that are 15°, 30°, and 45°. The E-field distribution is given in Fig. 11. As expected, the E-field strength inside the apartment decreases with increase of α. When α is 45°, the maximum value of E-field strength reaches the critical value of 12 V/m.

Due to the fact that many buildings are constructed of reinforced concrete, larger conductivities, namely 0.01 S/m and 0.1 S/m, are considered for the wall, ceiling and floor. Take the angle of 45° for example, the E-field distribution is shown in Fig. 12. It is obvious that the E-field strength also decreases with increase of conductivity and the maximum value of E-field strength goes down below 12 V/m.

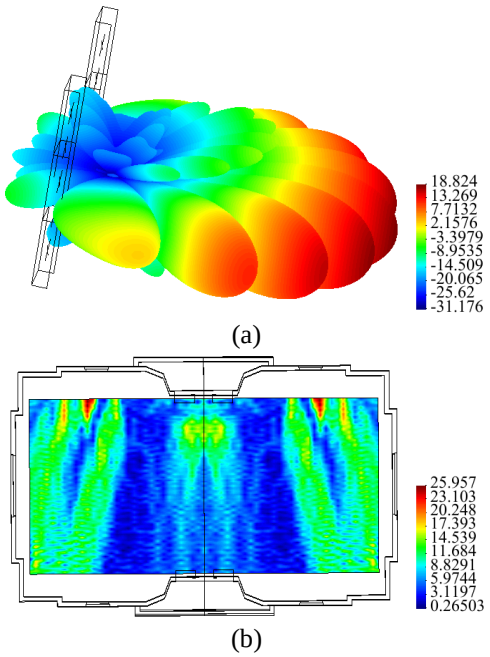

Fig. 9. Radiation pattern of the base-station antennas (a) and the E-field distribution on a cut-plane at a height of 1.70 m inside Apartment II (b).

Fig. 10. Main-lobe directions of base-station antennas in the *xoy* plane.

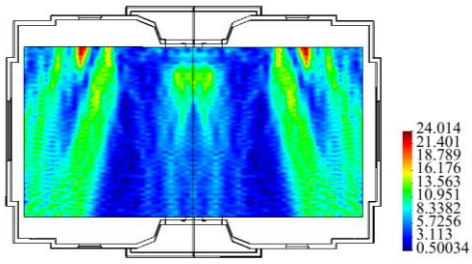

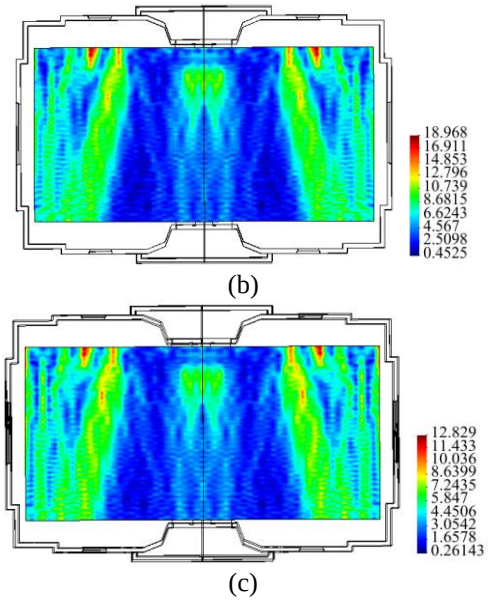

Fig. 11. E-field distribution generated by two base-station antennas with the azimuth angle of: (a) 15°, (b) 30° and (c) 45°. The cut-plane is at a height of 1.70 m inside Apartment II.

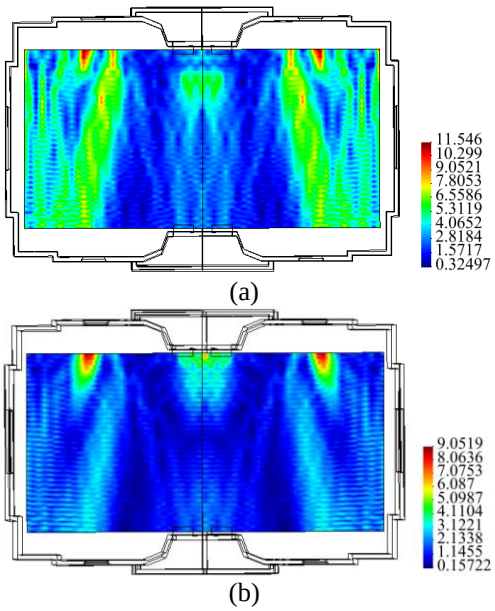

Fig. 12. E-field distribution generated by two base-station antennas with the conductivities of: (a) 0.01 S/m and (b) 0.1 S/m for the wall, ceiling and floor. The cut-plane is at a height of 1.70 m inside Apartment II.

V. CONCLUSION

We propose a parallel higher-order method of moments for assessing the indoor radiation level. The electric-field distribution is simulated inside three-dimensional buildings and the accuracy of the numerical simulations is confirmed by the measurements. Because different radiation safety standards are adopted in the world, one should use the local standard for assessment. The future work will focus on the improvement of the proposed method to simulate larger models, such as the electric-field distribution in a tall building.

ACKNOWLEDGMENT

This work is supported by the NSFC (61301069), the program for New Century Excellent Talents in University of China (NCET-13-0949), the Fundamental Research Funds for the Central Universities (JB160218), and the National High Technology Research and Development Program of China (863 Program) (2012AA01A308).

REFERENCES

[1] A. Bamba, W. Joseph, J. B. Andersen, E. Tanghe, G. Vermeeren, D. Plets, J. O. Nielsen, and L. Martens, "Experimental assessment of specific absorption rate using room electromagnetics," *IEEE Trans. Electromagn. Compat.*, vol. 54, no. 4, pp. 747-757, August 2012.

[2] O. Cerezci1, A. Y. Citkaya, S. S. Seker, and Z. S. Citkaya, "Determination of the electromagnetic pollution in a district and recommendations to decrease exposure levels," in *30th Annual Review of Progress in Applied Computational Electro-magnetics*, Jacksonville, USA, , pp. 697-702, 23-27 March 2014.

[3] K. A. Remley, H. R. Anderson, and A. Weisshar, "Improving the accuracy of ray-tracing techniques for indoor propagation modeling," *IEEE Trans. Veh. Technol.*, vol. 49, no. 6, pp. 2350-2358, November 2000.

[4] N. Tran-Minh and T. Do-Hong, "Application of raytracing technique for predicting average power distribution in indoor environment," in *Second International Conference on Communications and Electronics*, Hoi an, Vietnam, pp. 121-125, 4-6 June 2008.

[5] R. F. Harrington, *Field Computation by Moment Methods*, in IEEE Series on Electromagnetic Waves. New York: IEEE, 1993.

[6] K. S. Yee, "Numerical solution of initial boundary value problems involving Maxwell's equations in isotropic media," *IEEE Trans. Antennas Propag.*, vol. 14, no. 3, pp. 302-307, May 1966.

[7] A. Alighanbari and C. D. Sarris, "Parallel time-domain full-wave analysis and system-level modeling of ultrawideband indoor communication systems," *IEEE Trans. Antennas Propag.*, vol. 57, no. 1, pp. 231-240, January 2009.

[8] X. P. Yang, Q. Chen, and K. Sawaya, "Numerical analysis of wall effect on indoor MIMO channel capacity by using MoM-FDTD hybrid technique,"

in *Proc. IEEE Antennas Propag. Soc. Int. Symp.*, Albuquerque, USA, pp. 2979-2982, 9-14 July 2006.

[9] V. Pham-Xuan, I. Kavanagh, M. Condon, and C. Brennan, "On comparison of integral equation approaches for indoor wave propagation," in *IEEE-APS Topical Conference on Antennas and Propagation in Wireless Communications (APWC)*, Aruba, pp. 796-799, 3-9 August 2014.

[10] J. Fostier and F. Olyslager, "An asynchronous parallel MLFMA for scattering at multiple dielectric objects," *IEEE Trans. Antennas Propag.*, vol. 56, no. 8, pp. 2346-2355, August 2008.

[11] Ç. Kurnaz, "An empirical modeling of electromagnetic pollution on a university campus," *ACES Express Journal*, vol. 1, no. 2, pp. 76-79, February 2016.

[12] Y. Zhang and T. K. Sarkar, *Parallel Solution of Integral Equaton Based EM Problems in the Frequency Domain*. Hoboken, NJ: Wiley, 2009.

[13] B. M. Kolundzija and A. R. Djordjevic, *Electromagnetic Modeling of Composite Metallic and Dielectric Structures*. Norwood: Artech House, 2002.

[14] S. M. Rao, D. R. Wilton, and A. W. Glisson, "Electromagnetic scattering by surfaces of arbitrary shape," *IEEE Trans. Antennas Propag.*, vol. 30, no. 3, pp. 409-418, May 1982.

[15] Y. Zhang, Z. Lin, X. Zhao, and T. K. Sarkar, "Performance of a massively parallel higher-order method of moments code using thousands of CPUs and its applications," *IEEE Trans. Antennas Propag.*, vol. 62, no. 12, pp. 6317-6324, December 2014.

[16] http://www.feko.info/

[17] C. K. Chio, S.-W. Ting, X. W. Zhao, T. K. Sarkar, Y. Zhang, and K.-W. Tam, "Prediction model for radiation from base-station antennas using electromagnetic simulation," in *Proc. of Asia-Pacific Microwave Conference*, Kaohsiung, Taiwan, pp. 1082-1084, 4-7 December 2012.

[18] http://www.anite.com/businesses/network-testing